Skeletal Radiol (1987) 16:635–643

Skeletal Radiology

The role of magnetic resonance imaging in giant cell tumor of bone

Steven D. Herman, M.D.[1], Mamed Mesgarzadeh, M.D.[1], Akbar Bonakdarpour, M.D.[1], and Murray K. Dalinka, M.D.[2]

[1] Department of Diagnostic Imaging, Temple University Hospital, and
[2] Department of Radiology, Hospital of the University of Pennsylvania, Philadelphia, Pennsylvania, USA

Abstract. In six cases of giant cell tumor the magnetic resonance (MR) images obtained with various pulse sequences and field strengths were compared to the corresponding computed tomography (CT) scans and plain roentgenograms. MRI was superior to CT and plain films in demonstrating areas of tissue inhomogeneity within the tumor as well as soft tissue extension. CT was superior in demonstrating cortical thinning. Multiplanar imaging capability and visualization of articular cartilage may demonstrate intra-articular tumor spread. The characteristic MRI findings with short TR/TE (T1-weighting) and long TR/TE (T2-weighting) are described. We also describe one case where serial MR scans were used to assess response to therapy.

Key words: Giant cell tumor – Bone neoplasms – Magnetic resonance imaging

Although it is relatively new, magnetic resonance imaging is becoming an important modality in the evaluation of diseases of the musculoskeletal system. MRI's multiplanar capability, excellent soft tissue contrast, and lack of side effects have contributed to its effectiveness in evaluating bone tumors. MRI is useful in determining the extent of marrow and joint involvement and soft tissue extension. Because of its superior soft tissue contrast, MRI is the best modality for demonstrating tissue inhomogeneity. It can also be used to follow patients after radiation therapy. We have performed MRI in six patients with giant cell tumors using a variety of magnetic field strengths and pulse sequences. We compare the merits of MRI to those of CT and plain films in these six cases.

Address reprint requests to: Mamed Mesgarzadeh, M.D., Department of Diagnostic Imaging, Temple University Hospital, Broad and Ontario Streets, Philadelphia, PA 19140, USA

Material and methods

The authors have studied six patients with giant cell tumors. The patients ranged in age from 18 to 61 years; five were between 18 and 38. Four were females. Three of the lesions were around the knee, one was in the femoral neck, one was in the distal ulna, and one was in the sacrum. Plain films were available for comparison in all cases, and five patients had CT. Arthrography was available in one of the cases. Three patients were studied on a Fonar 0.3 Tesla resistive magnet, two were studied with a GE 0.13 Tesla resistive magnet, and one was studied with a GE 1.5 Tesla superconductive magnet. Body coils and a 256×256 matrix were used in all cases. Slice thicknesses, slice intervals, anatomic planes and pulse sequences are listed in Table 1.

Case reports

The radiological studies of three patients (4–6) were sent to us for review from other institutions. These cases were proven by biopsy, but the details of their clinical histories were not available. Therefore, only the radiological findings are described.

Case 1

An 18-year-old female presented with left knee pain after a sports injury. Radiographs revealed a classic giant cell tumor of the distal femur with a pathological fracture. The tumor extended to the subchondral bone (Fig. 1A). CT showed marked cortical thinning and minimal expansion (Fig. 1B). MRI showed replacement of the marrow by a tumor corresponding in size to the plain film abnormality (Fig. 1C). The sagittal and coronal images demonstrated no evidence of intra-articular extension. After healing of the fracture, the patient was treated with local curettage and bone grafting. Arthrography prior to surgery confirmed lack of joint involvement. The patient's postoperative course was uneventful.

Case 2

A 28-year-old male presented with a 5-month history of left groin pain following a "pulled groin muscle". Analgesics and

Table 1. Summary of the technical factors utilized in MR studies of each case

Case	Field strength (*T*)	Slice thickness/interval (mm)	Plane	Pulse sequences (TE/TR, TI/TR-ms)
1	0.3	9/1	Axial	SE 28/500, 28/2000, 56/2000
		4/3	Sagittal	SE 28/500, 28/2000
		4/3	Coronal	SE 28/556
2	0.3	9/1	Axial	SE 28/500, 56/2000
		4/3	Sagittal	SE 28/500
		4/3	Coronal	SE 28/500
3	0.3	9/1	Axial	SE 28/1000, 28/1500, 28/2000 IR 110/1500, 310/1500
			Sagittal	SE 28/1000
4	0.13	9/1	Axial	SE 12/150
			Coronal	SE 12/150
5	0.13	5/7	Coronal	SE 13/144
6	1.5	N/A	Axial	SE 25/400
			Coronal	SE 25/400, 40/2500, 80/2000

heat failed to alleviate the pain, and it grew progressively worse. Radiographs of the pelvis demonstrated a lytic lesion of the left femoral neck with a pathologic fracture (Fig. 2A). CT showed thinning and erosion of the bony cortex, but no evidence of soft tissue invasion. The MR assessment of the tumor's extent corresponded to the CT and plain film findings (Figs. 2C, D). The patient underwent a percutaneous needle biopsy of the femoral neck that revealed a giant cell tumor. He elected to have resection of the lesion with replacement by a femoral head prosthesis. His postoperative course was unremarkable.

Case 3

A 25-year-old woman presented with low back pain and bilateral sciatica which progressed over 4 months to incontinence and motor weakness. Past medical history was negative. On physical examination she had occult blood in the stool and hemoglobin was 9.5 gm. Plain films of the pelvis demonstrated a huge destructive mass involving both sides of the sacrum, L5, and both iliac bones (Fig. 3A). CT showed that most of the sacrum was destroyed, and massive anterior soft tissue extension had displaced the rectum. The MR images demonstrated a massive tumor invading the soft tissues and bone, and both contained some areas of heterogeneous signal intensity (Figs. 3B, C). An emergency lumbosacral decompression was performed, and biopsy at the time of surgery demonstrated giant cell tumor. The patient was treated with 5000 rads to the lumbosacral area. She developed weakness and recurrence of incontinence 10 months after therapy and required an additional 5000 rads. Serial MR scans since therapy have shown some increasing signal heterogeneity attributed to postradiation fibrosis, but no real change in tumor size (Fig. 3D).

Case 4

The plain films in this 61-year-old female showed a well-circumscribed lytic lesion in the lateral proximal right tibia (Fig. 4A). CT revealed no evidence of cortical breakthrough or soft tissue extension (Fig. 4B). The MR scan demonstrated an intramedullary tumor of the same extent shown on CT and plain films (Fig. 4C).

Case 5

The plain films in this 24-year-old female showed an ill-defined lesion of the lateral aspect of the proximal right tibia (Fig. 5A). CT demonstrated prominent soft tissue extension with obliteration of the cortical margin (Fig. 5B). The extension of the tumor into the soft tissue was more clearly seen on the MR images (Fig. 5C).

Case 6

Plain films showed that this 38-year-old male had a well-circumscribed lytic lesion of the distal left ulna (Fig. 6A). The ulnar styloid process was spared, and there was no evidence of cortical breakthrough. MRI corroborated the plain film findings of tumor extent (Fig. 6B). CT was not performed in this case.

Results

All modalites showed a similar intraosseous extent of tumor in all cases. In four cases, the tumor was well-circumscribed, and in two cases (3,5) there was prominent soft tissue invasion and cortical bone destruction. In each well-circumscribed case, with T1-weighted sequences, the tumors showed homogeneous diminished signals when compared to those from adjacent uninvolved marrow, an indication of prolonged T1 values (Figs. 1C, 2C, 4C, 6B). In all cases with T2 weighting, signals were isointense or hyperintense as compared to those from normal marrow indicating prolonged T2 values in the tumors (Figs. 1D, 2D). In case 3, there were areas of both high and low signal intensity on the T2-weighted images (Fig. 3C). In the first case, an intermediate pulse sequence SE (TE28, TR2000), neither predominantly T1- nor T2-weighted, produced a tumor signal which was in-

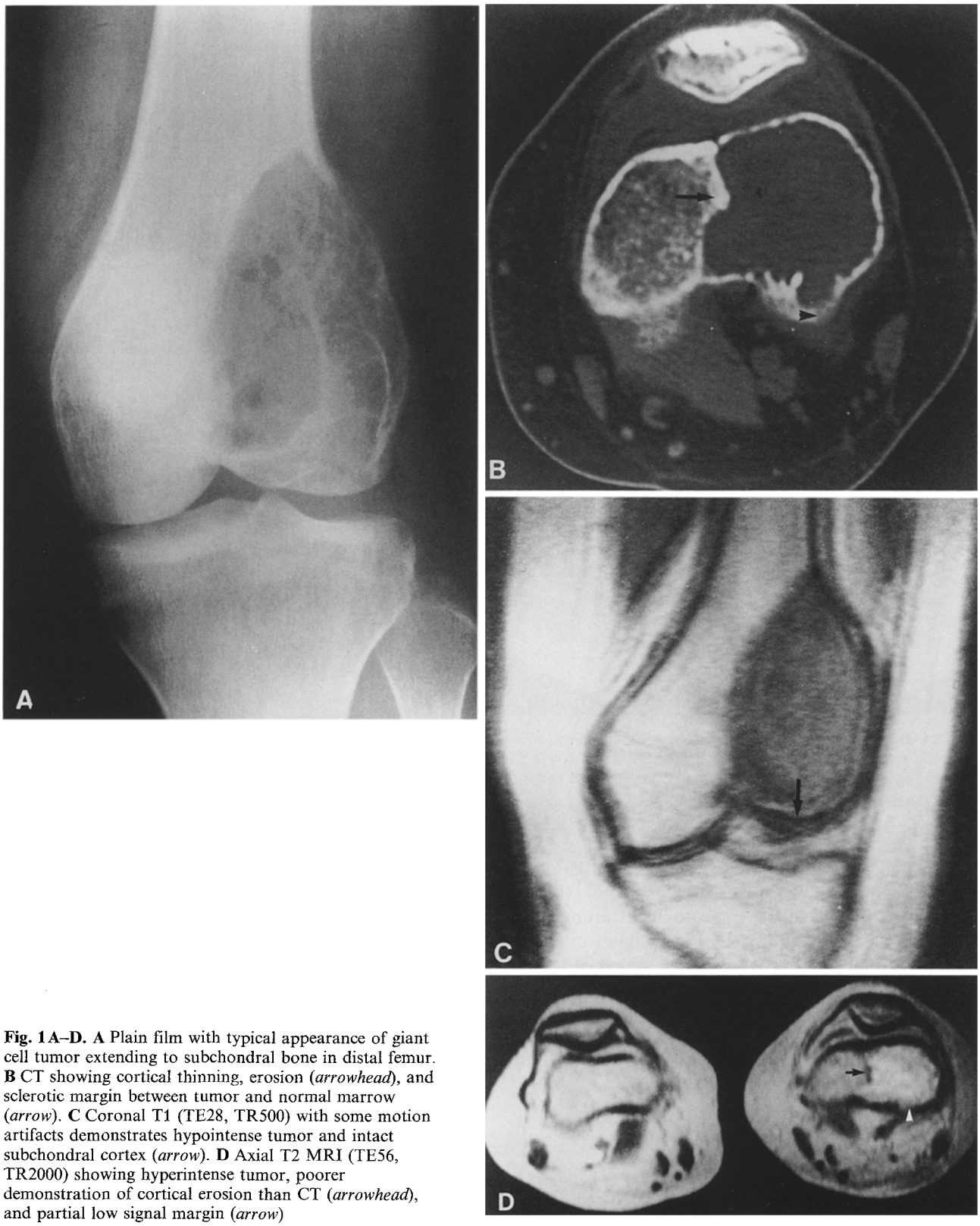

Fig. 1A–D. **A** Plain film with typical appearance of giant cell tumor extending to subchondral bone in distal femur. **B** CT showing cortical thinning, erosion (*arrowhead*), and sclerotic margin between tumor and normal marrow (*arrow*). **C** Coronal T1 (TE28, TR500) with some motion artifacts demonstrates hypointense tumor and intact subchondral cortex (*arrow*). **D** Axial T2 MRI (TE56, TR2000) showing hyperintense tumor, poorer demonstration of cortical erosion than CT (*arrowhead*), and partial low signal margin (*arrow*)

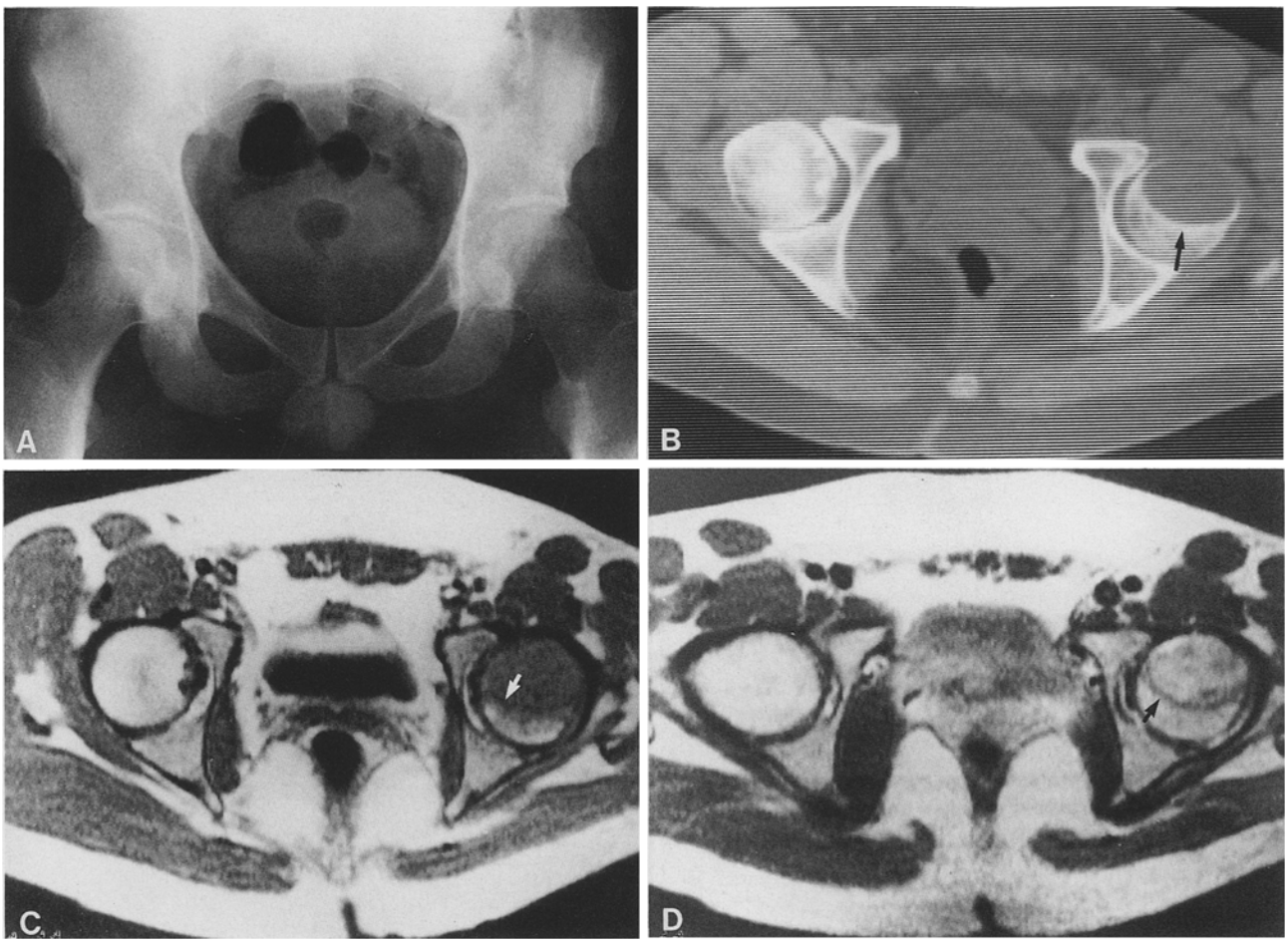

Fig. 2A–D. **A** Plain film shows a pathological fracture (*arrowhead*) in this femoral neck lesion. **B** CT showing marked cortical thinning and reactive sclerosis at margin (*arrow*). **C** Axial T1 MRI (TE28, TR500) showing low signal tumor and lower signal margin (*arrow*). **D** T2-weighted image (TE56, TR2000) better demonstrates the low signal margin than T1-weighted image (*arrow*), which corresponds to reactive sclerosis on CT

termediate in brightness between the T1 and T2 weighted images. In four cases (1, 2, 4, 6), the tumors were separated from the adjacent uninvolved bone marrow by a thin rim of low signal intensity similar to that of the cortical bone (Figs. 2D, 4C). In the two cases with extensive soft tissue spread, such low signal margins were not apparent. As one would expect, this feature was best seen on T2-weighted images owing to increased contrast between the brighter signal tumor and the low signal band (Fig. 2D).

Discussion

Before the advent of MRI, CT and arthrotomography were the best-known radiologic modalities for demonstrating soft tissue or intra-articular invasion by giant cell tumors [6, 8]. Due to their highly vascular nature, angiography has also been used before surgery to evaluate tumor size, soft tissue extension, and relationship with major vessels [5]. There are several reports concerning the role of MRI in evaluating bone tumors in general [1, 3, 7, 9, 10]. There is only one report (covering four cases) specifically dealing with MR imaging of giant cell tumor [2].

Zimmer et al. [10] consistently demonstrated significantly longer T1 and T2 relaxation times in a wide variety of skeletal neoplasms regardless of their benignity or malignancy. Therefore, these neoplasms produce lower signals on T1-weighted images and higher signals on T2-weighted images relative to the signal of normal marrow. In our cases, we also noted that tumor produced a lower signal relative to normal marrow on T1-weighted images regardless of the pulse sequence or field strength used. On the T2-weighted images, we found that, depending on the degree of T2 weighting, signals

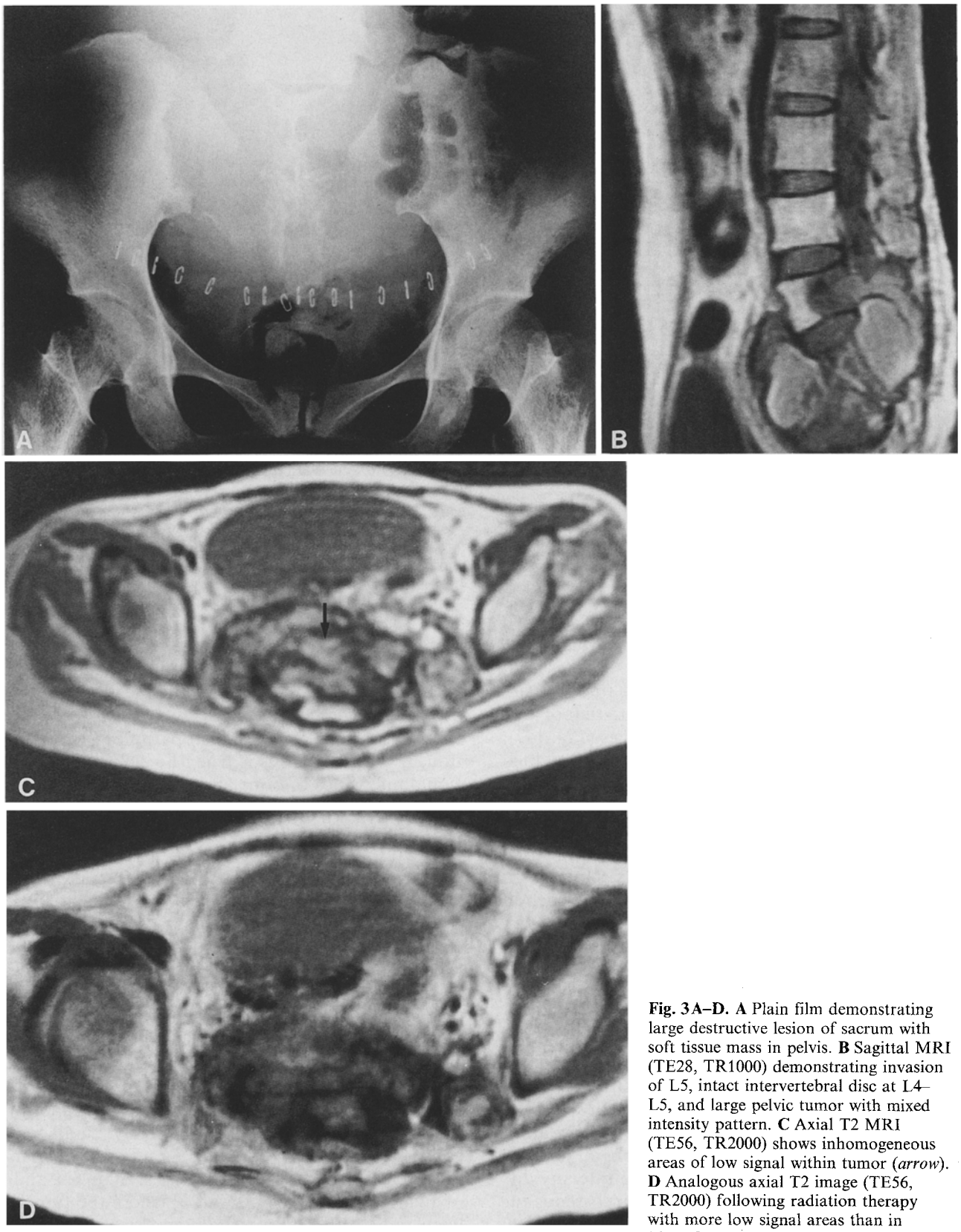

Fig. 3A–D. **A** Plain film demonstrating large destructive lesion of sacrum with soft tissue mass in pelvis. **B** Sagittal MRI (TE28, TR1000) demonstrating invasion of L5, intact intervertebral disc at L4–L5, and large pelvic tumor with mixed intensity pattern. **C** Axial T2 MRI (TE56, TR2000) shows inhomogeneous areas of low signal within tumor (*arrow*). **D** Analogous axial T2 image (TE56, TR2000) following radiation therapy with more low signal areas than in Fig. 3C

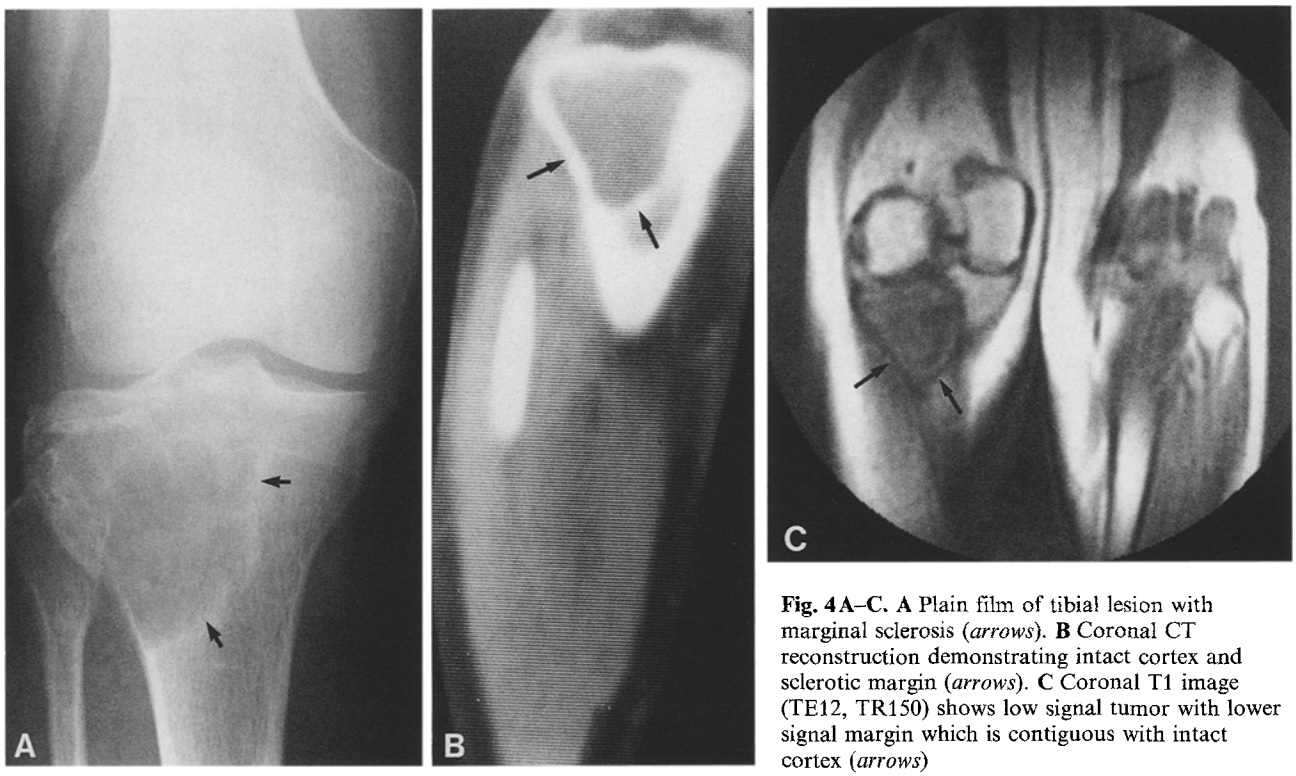

Fig. 4A–C. **A** Plain film of tibial lesion with marginal sclerosis (*arrows*). **B** Coronal CT reconstruction demonstrating intact cortex and sclerotic margin (*arrows*). **C** Coronal T1 image (TE12, TR150) shows low signal tumor with lower signal margin which is contiguous with intact cortex (*arrows*)

were either isointense or hyperintense relative to marrow. Involvement of medullary bone is best seen on T1-weighted images (Fig. 1C) since the signal intensity of tumor is almost equal to that of normal marrow fat on T2-weighted images (Fig. 1D).

Cortical invasion is best seen on T2-weighted images in which the normally black cortical bone may be focally replaced by higher intensity tumor (Fig. 1D). With increased T2-weighting, the tumor signal brightens and the level of this contrast grows. However, CT remains clearly superior to MR for demonstrating subtle cortical destruction because MRI has (a) poorer spatial resolution, (b) limited ability to demonstrate mineralized structures, and (c) increased motion artifact due to prolonged acquisition time, particularly with T2 imaging.

Due to its increased soft tissue contrast, MR is superior to CT in demonstrating extraosseous extension of tumor (Figs. 3B, 5C). Although muscle and tumor may have similar densities on CT, the inherent differences in T1 and T2 relaxation times between muscle and tumor can be demonstrated with MR. We did not demonstrate any difference in signal intensity between intraosseous tumor and extraosseous extension. In Zimmer's series, higher signals were found in those portions of tumor in the surrounding soft tissues. Zimmer attributed the difference to the possible presence of low signal bone admixed with the tumor cells within the medullary cavity, while the extraosseous extension consisted of purely tumor cells. We feel that this claim requires histopathologic correlation. If this hypothesis is true, the lack of different signal intensities of bone and giant cell tumor may be due to the fact that the intraosseous and extraosseous lesions are composed purely of tumor cells without matrix production.

In the three cases studied with coronal and/or sagittal imaging, the joint itself was thought to be free of tumor (Fig. 1C). This lack of intra-articular spread was surgically confirmed in each case. The multiplanar imaging capability of MRI may prove to be useful in determining joint involvement, although the number of cases in this series is too small to yield a definitive conclusion.

In four of our cases (cases 1, 2, 4 and 6) the margin of the tumor was partially or completely separated from the surrounding normal spongy bone by a band of low signal intensity. In all four cases, this band corresponded to an area of marginal sclerosis of varying thickness seen on CT and/or plain films. In cases 3 and 5, where the tumors were radiographically more aggressive, this band of low signal was not present on MRI, nor was there a sclerotic margin on either the CT or plain

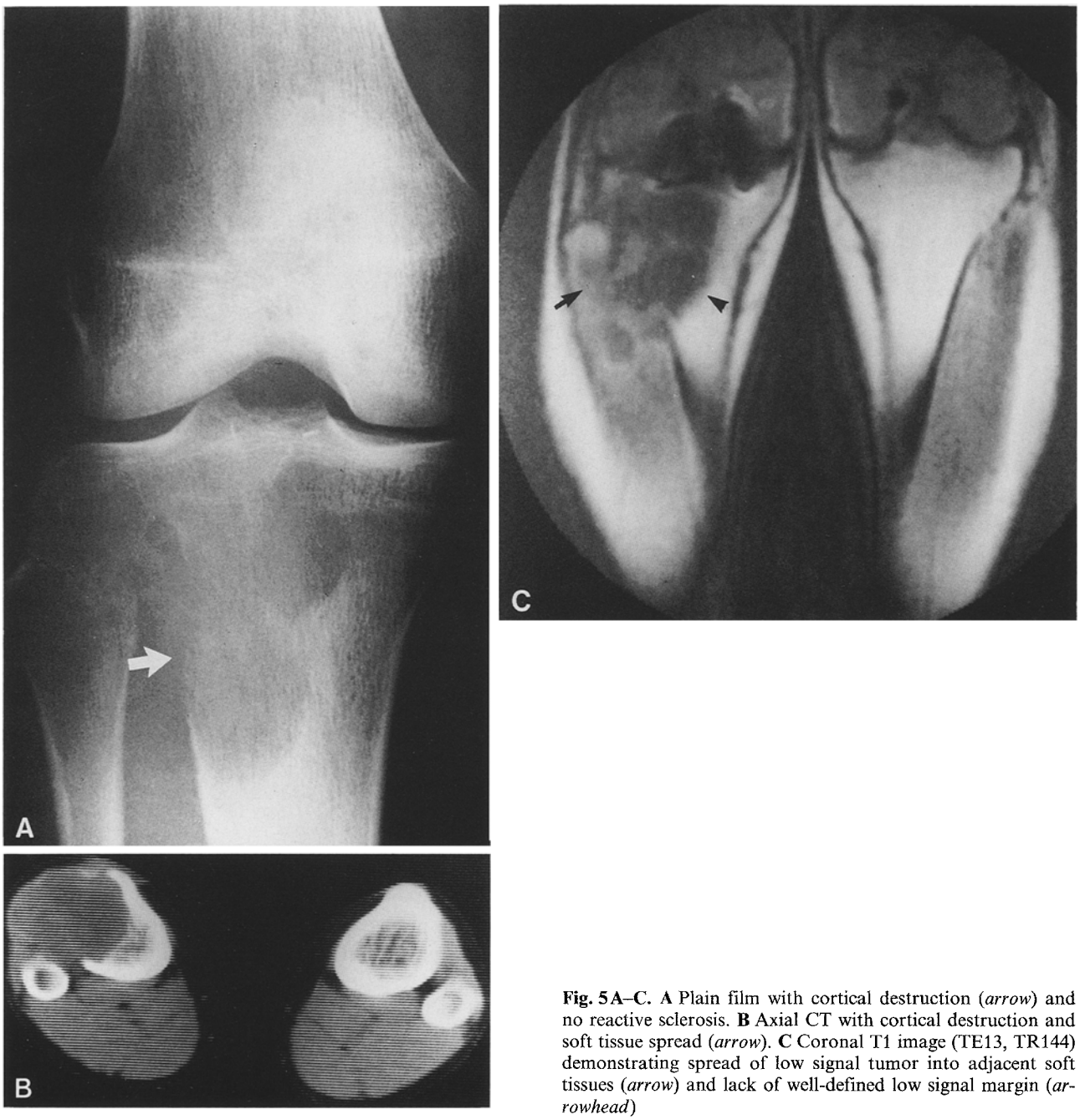

Fig. 5A–C. **A** Plain film with cortical destruction (*arrow*) and no reactive sclerosis. **B** Axial CT with cortical destruction and soft tissue spread (*arrow*). **C** Coronal T1 image (TE13, TR144) demonstrating spread of low signal tumor into adjacent soft tissues (*arrow*) and lack of well-defined low signal margin (*arrowhead*)

radiographs. Our series is too small to draw a definite conclusion; however, since bony sclerosis is a host reaction against the tumor and correlates with a less aggressive radiographic appearance, a better prognosis might be predicted when the tumor is contained within this band of low signal intensity. This sharp, smooth, well-defined border of low signal has also been described in other osseous tumors; however, no correlation has been made with the presence or absence of bony sclerosis. It has been concluded that this finding strongly suggests benignity, an explanation that concurs with our hypothesis [10].

In our series, the most radiographically aggressive tumor (case 3) demonstrated areas of decreased signal within the otherwise hyperintense tumor on T2-weighted images. This was most probably due to areas of tissue inhomogeneity, a common finding in aggressive giant cell tumors [4]. These areas of inhomogeneity were not visible on

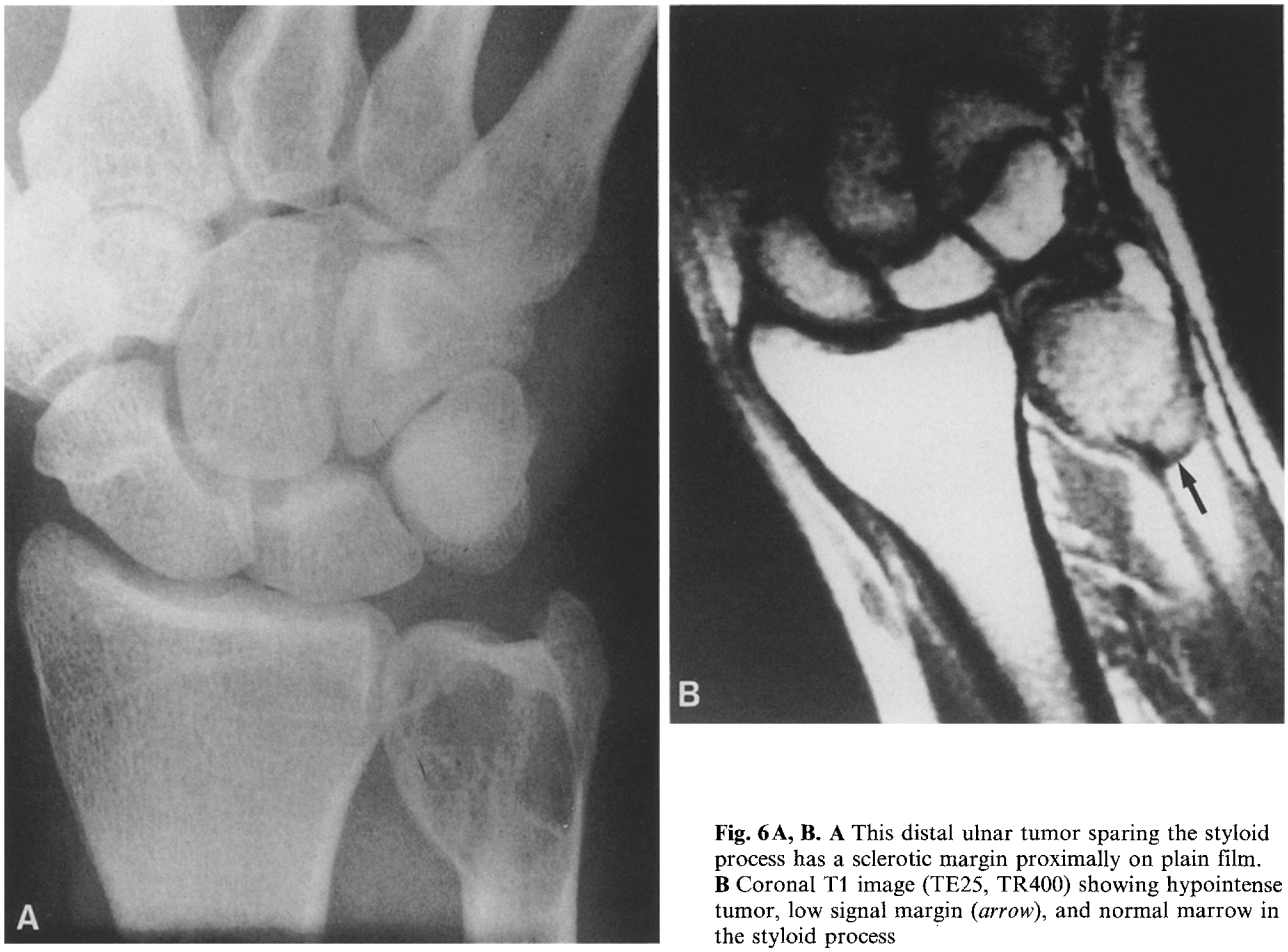

Fig. 6A, B. **A** This distal ulnar tumor sparing the styloid process has a sclerotic margin proximally on plain film. **B** Coronal T1 image (TE25, TR400) showing hypointense tumor, low signal margin (*arrow*), and normal marrow in the styloid process

the T1-weighted images. Areas of inhomogeneity within tumors have been attributed to areas of hemorrhage and/or necrosis in those sites which do not contain tumor calcification. Other investigators have concluded that the presence of inhomogeneities within a tumor is a strong indication of malignancy [10], and this concurs with the aggressive nature of our case.

Despite the good correlation between sclerotic rim and areas of tissue inhomogeneity with the resultant MR signal patterns, we question the significance of these findings in the case of giant cell tumor. These tumors are notorious for their unpredictable clinical behavior on the basis of their histology [4]. Further studies and longer clinical follow-ups would be required to determine the true value of these findings. Serial MRI scans can provide valuable information in assessing the response of a tumor treated with radiation therapy by serial scanning because they reveal increasing amounts of inhomogeneous low signal intensity within the tumor that might result from postradiation fibrosis. It might also be possible to detect decreasing tumor bulk. In our case 3, even though the tumor size has not changed during one year since treatment the T2-weighted images contain more low signal areas, a finding compatible with the development of fibrosis.

In managing giant cell tumors, we conclude that MRI has some advantages over CT. However, neither modality adds anything to plain films in establishing the diagnosis of giant cell tumor. The role of MRI seems to be limited to preoperative evaluation of tumor extent, and possibly, to follow-up of those exceptional patients treated with radiation therapy.

Acknowledgements. We wish to thank Mr. Milne Hewish for photography and Mrs. Milena Herman and Mrs. Joyce S. Ragin for manuscript preparation.

References

1. Bloem JL, Falke THM, Taminian AHM, Doornbos J, Van Oosterom AT, Steiner RM, Overbosch EEH, Ziedses des

Plantes BG Jr (1985) Magnetic resonance imaging of primary malignant bone tumors. Radiographics 5:853
2. Brady TJ, Gebhardt MC, Pykett IL, Buonanno FS, Newhouse JH, Burt CT, Smith RJ, Mankin HJ, Kistler JP, Goldman MR, Hinshaw WS, Pohost GM (1982) NMR imaging of forearms in healthy volunteers and patients with giant cell tumor of bone. Radiology 144: 549
3. Brady TJ, Rosen BR, Pykett IL, McGuire MH, Mankin, HJ, Rosenthal DI (1983) NMR imaging of leg tumors. Radiology 149:181
4. Dahlin DC (1985) Giant cell tumor of bone: Highlights of 407 cases. AJR 144:955
5. Hudson, TM, Enneking WF, Hawkins IF Jr (1981) The value of angiography in planning surgical treatment of bone tumors. Radiology 138:283
6. Hudson TM, Schiebler M, Springfield DS, Enneking WF, Hawkins IF Jr, Spanier SS (1984) Radiology of giant cell tumors of bone: computed tomography, arthrotomography, and scintigraphy. Skeletal Radiol 11:85
7. Hudson TM, Hamlin DJ, Enneking WR, Pettersson H (1985) Magnetic resonance imaging of bone and soft tissue tumors: early experience in 31 patients compared with computed tomography. Skeletal Radiol 13:134
8. Levine E, DeSmet AA, Neff JR (1984) Role of radiologic imaging in management planning of giant cell tumor of bone. Skeletal Radiol 12:79
9. Richardson ML, Kilcoyne RF, Gillespy T, Helms CA, Genant HK (1986) Magnetic resonance imaging of musculoskeletal neoplasms. Radiol Clin North Am 24:259
10. Zimmer WD, Berquist TH, McLeod RA, Sim FH, Pritchard DJ, Shives TC, Wold LE, May GR (1985) Bone tumors: Magnetic resonance imaging versus computed tomography. Radiology 155:709